

Molecular modeling, structural analysis and identification of ligand binding sites of trypanothione reductase from *Leishmania mexicana*

Ozal Mutlu

Marmara University, Faculty of Arts and Sciences, Department of Biology, Istanbul, Turkey

ABSTRACT

Background & objectives: Trypanothione reductase (TR) is a member of FAD-dependent NADPH oxidoreductase protein family and it is a key enzyme which connects the NADPH and the thiol-based redox system. Inhibition studies indicate that TR is an essential enzyme for parasite survival. Therefore, it is an attractive target enzyme for novel drug candidates. There is no structural model for TR of *Leishmania mexicana* (*Lm*TR) in the protein databases. In this work, 3D structure of TR from *L. mexicana* was identified by template-based *in silico* homology modeling method, resultant model was validated, structurally analyzed and possible ligand binding pockets were identified.

Methods: For computational molecular modeling study, firstly, template was identified by BLAST search against PDB database. Multiple alignments were achieved by ClustalW2. Molecular modeling of *Lm*TR was done and possible drug targeting sites were identified. Refinement of the model was done by performing local energy minimization for backbone, hydrogen and side chains. Model was validated by web-based servers.

Results: A reliable 3D model for TR from *L. mexicana* was modeled by using *L. infantum* trypanothione reductase (*Li*TR) as a template. RMSD results according to C-alpha, visible atoms and backbone were 0.809 Å, 0.732 Å and 0.728 Å respectively. Ramachandran plot indicates that model shows an acceptable stereochemistry.

Conclusion: Modeled structure of *Lm*TR shows high similarity with *Li*TR based on overall structural features like domains and folding patterns. Predicted structure will provide a source for the further docking studies of various peptide-based inhibitors.

Key words Homology modeling; *Leishmania mexicana*; thiol metabolism; trypanothione reductase

INTRODUCTION

Trypanosomatid protozoan parasites comprise genus of *Trypanosoma* and *Leishmania* that cause neglected tropical diseases. Leishmaniasis is seen frequently in 88 countries on four continents (Southeast Asia, Africa, South America including mostly Brazil and Mediterranean countries) and cause 1.6 million new cases annually¹. Leishmaniasis is transmitted by infected female sandflies to the vertebrate hosts and reproduces within macrophages. Three clinical forms of leishmaniasis are: cutaneous leishmaniasis (*L. major*, *L. tropica* and *L. mexicana*); visceral leishmaniasis (*L. donovani* and *L. infantum*) and mucocutaneous leishmaniasis (*L. braziliensis*) are seen in human hosts^{2, 3}.

Like other trypanosomatids, *L. mexicana* has no genes for glutathione reductase (GR), thioredoxin reductase (TrxR), catalase and selenocysteine-containing glutathione peroxidase which are responsible for intracellular thiol redox homeostasis in mammals⁴. Parasites have dithiol trypanothione [T(SH)₂] and trypanothione reductase (TR) in their redox metabolisms which are common for all trypanosomatids but absent in hosts^{5, 6}.

Trypanosomatids are exposed to reactive oxygen (superoxide anion radical, hydrogen peroxide, peroxynitrite and the hydroxyl radical) and nitrogen molecules that are originated from parasite itself as by-product of aerobic metabolism or from the host macrophage defense system^{5, 7}. Elimination of the various hydroperoxidases occurs via an electron transfer cascade which contains the enzymes of trypanothione, trypanothione reductase, tryparedoxin and tryparedoxin peroxidase⁶. These low molecular mass thiols and redox enzymes protect enzymes from reactive derivatives and facilitate adaptation to various metabolic and environmental conditions⁵.

One of the low molecular mass thiol compound is trypanothione [T(SH)₂] which is synthesized from two GSH and one spermidine molecule by glutathionyl spermidine/trypanothione synthetase (TryS) enzyme, an ATP driven reaction⁴. Trypanothione reductase uses NADH as an electron donor for the reduction of trypanothione disulfide to trypanothione. Because of lacking of GR and TrxR in trypanosomatids, TR is a key enzyme which connects the NADPH and the thiol-based redox system⁵. Trypanothione reductase knock out studies on *L. donovani* and *L. major* show decreased capacity to survive inside

host macrophages^{8, 9}. Conditional knock out studies on *T. brucei* resulted with growth arrest, loss of viability and virulence¹⁰. Inhibition studies showed that numerous compounds inhibit trypanosomatid TR but not inhibit host GR^{11–14}. These works indicate that TR is an essential enzyme for parasite survival⁶. So, TR is an attractive target enzyme for novel drug candidates because of the absence of trypanothione redox system in mammals^{15–17}.

Trypanothione reductase is a member of FAD-dependent NADPH oxidoreductase protein family and shares close structural similarities with GR, lipoamide dehydrogenase and eukaryotic TrxRs⁵. It has a mass of 52 kDa, comprises of a FAD and NADPH binding, central and interface domains and has two active sites. Structural features of TR from trypanosomatids and crystal structures of TR from *T. cruzi*^{18,19}, *Crithidia fasciculata*²⁰ and *L. infantum*²¹ were solved. However, there is no 3D model for TR of *L. mexicana* (*LmTR*) in the protein databases. In this work, *in silico* homology modeling approach was used to determine 3D model of TR from *L. mexicana*, model was validated by web-based tools, structure was analyzed and possible drug target pockets were identified.

MATERIAL & METHODS

Template selection and multiple sequence alignment

The National Center for Biotechnology Information (<http://www.ncbi.nlm.nih.gov>) database was used to obtain amino acid sequence of the target TR from *L. mexicana* (*LmTR*) (MHOM/GT/2001/U1103) with the accession number of CBZ23392. Template identification was done by NCBI BLAST tool and two types of BLAST (Basic Local Alignment Search Tool), protein-protein BLAST and PSI-BLAST (Position Specific Iterated-BLAST) were performed for template selection against database Protein Data Bank (PDB) proteins. Homolog structure having the best score was selected as a template protein after comparative searching. Template protein PDB file and amino acid sequence in FASTA format was downloaded from the PDB (<http://www.rcsb.org/pdb/home/home.do>). Multiple sequence alignment was performed by both Molsoft and ClustalW2²² from the European Bioinformatics Institute.

Homology model development and validation

A 3D model for the *LmTR* enzyme was built by Molsoft ICM. Knowledge from the target sequence, alignment and 3D structure of the template protein which was obtained from the PDB was used to construct the model. Refinement of the obtained model was achieved by performing local energy minimization for backbone, hydro-

gen and side chains. Secondary structure of the protein was estimated by web-based program SOPMA²³.

Validation of the resultant protein model was achieved by checking stereochemistry, energy profile and residue environment. RAMPAGE Server²⁴ was used to check stereochemistry of the model. Model quality was analyzed by ProSA²⁵ and Protein Structure Validation Suite—PSVS 1.3 (http://psvs-1_4-dev.nesg.org). Statistics of non-bonding interactions was performed by ERRAT Server v.2.0²⁶. Physical and chemical parameters for the modeled protein (molecular weight, theoretical pI, amino acid composition, extinction coefficient, aliphatic index and grand average of hydropathicity) were performed by ProtParam tool²⁷.

Ligand binding site identification

Possible ligand binding sites/pockets on the 3D structure of protein were identified by Molsoft-ICM PocketFinder, web-based servers of CASTp-computer atlas of surface topography of proteins²⁸ and GHECOM 1.0: Grid-based HECOMi finder²⁹.

RESULTS & DISCUSSION

Template selection and multiple sequence alignment

BLAST searching of the TR from *L. mexicana* (*LmTR*) was performed against PDB proteins. The four top scores were from *L. infantum* (PDB number: 2JK6, Max score: 932, Identity: 91%, E-value: 0); *C. fasciculata* (PDB number: 1FEA, Max score: 832, Identity: 80%, E-value: 0); *T. cruzi* (PDB number: 1NDA, Max score: 686, Identity: 68%, E-value: 0); and *T. brucei* (PDB number: 2WBA, Max score: 686, Identity: 66%, E-value: 0). Evolutionary tree showed these proteins have closely related amino acid compositions. Sequence identity above 50% is ideal for structure-based drug design and target assessment, site directed mutagenesis and assignment of protein function³⁰. Therefore, according to the identity, max score and E-value, the closest enzyme sequence was from *L. infantum* (PDB 2JK6) that was selected as a template for *in silico* homology modeling. Figure 1 shows multiple sequence alignments of the TR from *L. mexicana* (*LmTR*), *L. infantum* (*LiTR*), *C. fasciculata* (*CfTR*), *T. brucei* (*TbTR*) and *T. cruzi* (*TcTR*) enzymes based on evolutionary tree. Multiple sequence alignment results showed that identity between *LmTR* and *LiTR* is 90%, *CfTR* is 80%, *TcTR* is 67%, and *TbTR* is 65% which were nearly same as that of BLAST search results.

Homology model development and validation

Trypanothione reductase from *L. mexicana* was mod-

Overall structure

Secondary structure of TR from *L. mexicana* was predicted by SOPMA server. As a result, random coils (33.2%) and alpha helices (33.6%) are dominant features. Extended strands and beta turns have found as 24.85 and 8.35% respectively (Fig. 3). Crystal structure of TR from *L. infantum*²¹, *C. fasciculata*²⁰ and *T. cruzi*^{18, 19} were solved. According to these studies all the TRs share three domains; FAD binding domain, NADPH binding domain and interface domain which are responsible in forming dimer state²¹ (Fig. 2). Catalytic site comprises redox active disulfide bridge (Cys52–Cys57 in *L. infantum* and Cys53–Cys58 in *T. cruzi*) and an active site base (His461) of the interface domain^{19, 21}. In *LmTR* redox active residues, active site bases are found in the positions Cys52–Cys57 and His461 like those found in *L. infantum* TR and Cys52–Cys57 form a disulfide bond about 2.2 Å distance (2.05 Å in *LiTR*) (Fig. 4). FAD domain consists five stranded parallel beta sheets (7–10, 31–35, 119–124,

155–158 and 322–324), three stranded antiparallel beta sheets (126–129, 134–138 and 149–152) and four alpha helices (14–26, 50–78, 92–116 and 335–349). NADPH domain contains three stranded antiparallel, three parallel beta sheets and two alpha helices. Interface domain located after the residue 360 to the end of the structure which contains four stranded antiparallel beta sheets and one alpha helix. NADPH binding domain residues (Tyr221, Arg222, Arg228/229, Tyr198, Ile199, Met333, Ala365 and Glu202/203) found in *LiTR* and *TcTR* well-preserved in the *LmTR*. These analyses show that the overall fold of *LmTR* highly resemble to those of other TRs' crystal structures. According to the active site and pocket prediction results, eight different pockets were identified by Molsoft ICM and 10 were from CASTp-computer atlas of surface topography of proteins and 13 were from GHECOM 1.0: Grid-based HECOMi finder. Results from Molsoft are given in Fig. 4 and Table 1. Pockets (Number 1 and 4) occupy the area of NADPH

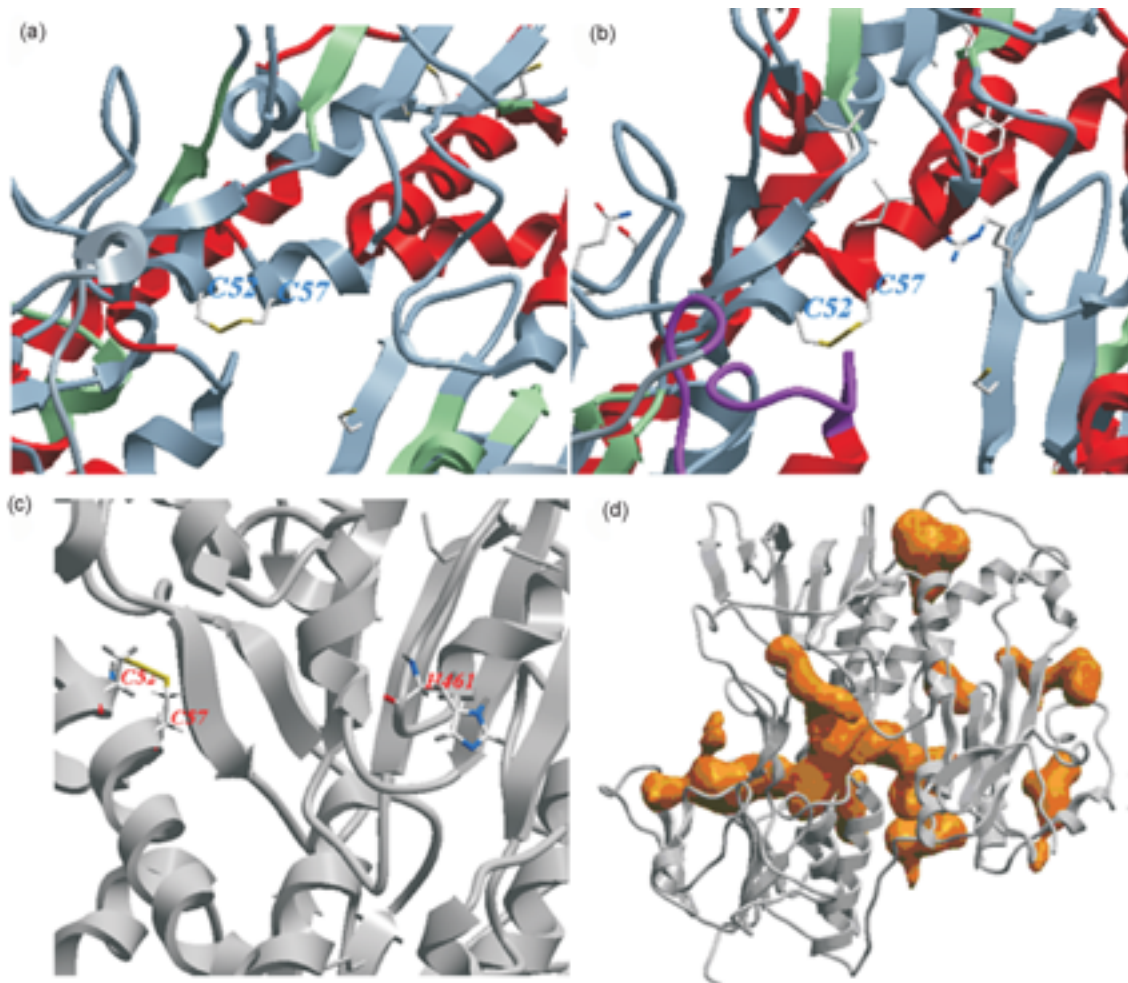


Fig. 4: (a) Disulfide bridge (C52–C57) region of the *LiTR*; (b) Disulfide bridge (C52–C57) region of the *LmTR*; (c) Active site residues (C52–C57 and H461) of the modeled *LmTR* enzyme; and (d) Predicted ligand binding pockets by icmPocketFinder (Molsoft ICM) for *LmTR*; Total enzyme structure was represented as grey and pockets are in orange.

Table 1. Identified volume, area and residue information of possible ligand binding pockets.

Pocket No.	Volume (AAA)	Area(AA)	Pocket residues
1	1565.2	1396.1	I10: [^] G16, [^] V34: [^] L36, [^] L44, [^] A46: [^] A47, [^] G50: [^] C52 , [^] V55: [^] V58, [^] K60: [^] K61, [^] G125: [^] A128 [^] R138, [^] S140: [^] E141, [^] Q143, [^] A159: [^] W163, [^] S178, [^] F182, [^] Y198 : [^] I199 , [^] F203, [^] F230, [^] R287, [^] R290, [^] Q292: [^] Q295, [^] I325: [^] V328, [^] M333 : [^] A338, [^] N340, [^] T357: [^] D358, [^] T360: [^] F367, [^] P435, [^] I438: [^] Q439, [^] G442: [^] I443, [^] K446
2	324.355	304.9	G66: [^] A67, [^] Y69: [^] M70, [^] L73: [^] R74, [^] R85, [^] L88: [^] S90, [^] G209: [^] R213"
3	234.547	278.676	F396, [^] P398: [^] H401, [^] K409, [^] F411, [^] G431: [^] S433, [^] H461 : [^] S464, [^] E466: [^] E467
4	224.235	269.759	[^] L167, [^] V194: [^] I199, [^] Y221 : [^] R222 , [^] L227: [^] R228 , [^] S254: [^] P255, [^] A284: [^] R287
5	167.787	216.276	[^] S440: [^] V441, [^] C444, [^] M447, [^] A449, [^] D453: [^] F454, [^] T457, [^] G459: [^] V460, [^] T463, [^] A465: [^] E466, [^] L468: [^] C469
6	142.982	171.104	[^] G229: [^] F230, [^] H359: [^] V362, [^] C364, [^] T374: [^] T378, [^] H428
7	129.093	138.48	[^] S14, [^] L17: [^] E18, [^] W21, [^] V53, [^] Y110, [^] M113, [^] T335, [^] I339
8	116.639	145.139	[^] K61, [^] V64: [^] T65, [^] Q68, [^] F367: [^] I369, [^] P371, [^] S433, [^] P435: [^] E436

Residues with bold type indicate active site (C52 and H461) and NADPH binding (Y198, I199, M333, Y221, R222 and R228) residues.

binding site that comprises of Tyr198, Ile199, Met333, Tyr221, Arg222 and Arg228 residues where pocket 1 and 3 occupy the region of the active site residues (Cys52 and His461) found.

CONCLUSION

Although all *Leishmanias* share a unique thiol-based metabolism which is common to all trypanosomatide family members, human hosts lack this antioxidant mechanism. Hence, enzymes of thiol-metabolism are subjected for drug design studies. Trypanothione reductases catalyse the transfer of electrons from the cofactor of NADPH to trypanothione substrate by the action of FAD and cysteine disulfides. In this computational modeling study, 3D structure of TR from the *L. mexicana* was solved for the first time by using crystal structure coordinates from *LiTR* which shares 90% amino acid sequence identity. Quality of the 3D structure of the model was confirmed by various web-based programs. Modeled structure of *LmTR* showed high similarity with *LiTR* based on overall structural features like domains and folding patterns. Structure could provide a good model for further structural-based drug design and docking studies of various peptide-based inhibitors.

REFERENCES

1. First WHO report on neglected tropical diseases: Working to overcome the global impact of neglected tropical diseases. In: Crompton DVT, editor. Leishmaniasis. Geneva: WHO Press 2010; p. 92.
2. Pavli A, Maltezos HC. Leishmaniasis, an emerging infection in travelers. *Int J Infect Dis* 2010; 14: 1032–9.
3. Desjeux P. The increase in risk factors for leishmaniasis worldwide. *Trans R Soc Trop Med Hyg* 2001; 95: 239–43.
4. Flohe L, Hecht H, Steinert P. Glutathione and trypanothione in parasitic hydroperoxide metabolism. *Free Radic Biol Med* 1999; 27: 966–84.
5. Krauth-Siegel RL, Comini MA. Redox control in trypanosomatids, parasitic protozoa with trypanothione-based thiol metabolism. *Biochim Biophys Acta* 2008; 1780: 1236–48.
6. Müller S, Liebau E, Walter RD, Krauth-Siegel RL. Thiol-based redox metabolism of protozoan parasites. *Trends Parasitol* 2003; 19 (7): 320–8.
7. Assche T, Deschacht M, Van da Luz RA, Maes L, Cos P. Leishmania–macrophage interactions: Insights into the redox biology. *Free Radic Biol Med* 2011; 51: 337–51.
8. Dumas C, Ouellette M, Tovar J, Cunningham ML, Fairlamb AH, Tamar S, et al. Disruption of the trypanothione reductase gene of *Leishmania* decrease its ability to survive oxidative stress in macrophages. *EMBO J* 1997; 16: 2590–8.
9. Tovar J, Wilkinson S, Mottram JC, Fairlamb AH. Evidence that trypanothione reductase is an essential enzyme in *Leishmania* by targeted replacement of the *TRYA* gene locus. *Mol Microbiol* 1998; 29: 653–60.
10. Krieger S, Schwarz W, Ariyanayagam MR, Fairlamb AH, Krauth-Siegel RL, Clayton C. Trypanosomes lacking trypanothione reductase are avirulent and show increased sensitivity to oxidative stress. *Mol Microbiol* 2000; 35(3): 542–52.
11. Benson TJ, McKie JH, Garforth J, Borges A, Fairlamb AH, Douglas KT. Rationally designed selective inhibitors of trypanothione reductase phenothiazines and related tricyclics as lead structures. *Biochem J* 1992; 286: 9–11.
12. Blumenstiel K, Schöneck R, Yardley V, Croft SL, Krauth-Siegel RL. Nitrofurans as common subversive substrates of *Trypanosoma cruzi* lipoamide dehydrogenase and trypanothione reductase. *Biochem Pharma* 1999; 58: 1791–9.
13. Bonnet B, Soulez D, Davioud-Charvet E, Landry V, Horvath D, Sergheraert C. New spermine and spermidine derivatives as potent inhibitors of *Trypanosoma cruzi* trypanothione reductase. *Bioorg Med Chem* 1997; 5(7): 1249–56.
14. Krauth-Siegel RL, Inhoff O. Parasite-specific trypanothione reduc-

- tase as a drug target molecule. *Parasitol Res* 2003; 90: 77–85.
15. Krauth-Siegel RL, Bauer H, Schirmer RH. Dithiol proteins as guardians of the intracellular redox milieu in parasites: Old and new drug targets in trypanosomes and malaria-causing plasmodia. *Angew Chem Int Ed Engl* 2005; 44: 690–715.
 16. Jaeger T, Flohé L. The thiol-based redox networks of pathogens: Unexploited targets in the search for new drugs. *Biofactors* 2006; 27: 109–20.
 17. Piñeyro MD, Parodi-Talice A, Arcari T, Robello C. Peroxiredoxins from *Trypanosoma cruzi*: Virulence factors and drug targets for treatment of Chagas disease. *Gene* 2008; 408: 45–50.
 18. Lantwin CB, Schlichting I, Kabsch K, Pai EF, Krauth-Siegel RL. The structure of *Trypanosoma cruzi* trypanothione reductase in the oxidised and NADPH reduced state. *Proteins Struct Funct Genet* 1994; 18: 161–73.
 19. Zhang Y, Bond CS, Bailey S, Cunningham ML, Fairlamb AH, Hunter WN. The crystal structure of trypanothione reductase from the human pathogen *Trypanosoma cruzi* at 2.3 Å resolution. *Protein Sci* 1996; 5: 52–61.
 20. Kuriyan J, Kong XP, Krishna TS, Sweet RM, Murgolo NJ, Field H, et al. X-ray structure of trypanothione reductase from *Crithidia fasciculata* at 2.4 Å resolution. *Proc Natl Acad Sci* 1991; 88: 8764–8.
 21. Baiocco P, Colotti G, Franceschini S, Ilari A. Molecular basis of antimony treatment in Leishmaniasis. *J Med Chem* 2009; 52(8): 2603–12.
 22. Larkin MA, Blackshields G, Brown NP, Chenna R, McGettigan PA, McWilliam H, et al. Clustal W and Clustal X version 2.0. *Bioinformatics* 2007; 23: 2947–8.
 23. Geourjon C, Deleage G. SOPMA: Significant improvements in protein secondary structure prediction by consensus prediction from multiple alignments. *Comput Appl Biosci* 1995; 11(6): 681–4.
 24. Lovell SC, Davis IW, Arendall WB, de Bakker PIW, Word JM, Prisant MG, et al. Structure validation by C-alpha geometry: Phi, psi and C-beta deviation. *Proteins Struct Funct Genet* 2002; 50: 437–50.
 25. Wiederstein M, Sippl MJ. ProSA-web: Interactive web service for the recognition of errors in three-dimensional structures of proteins. *Nucleic Acid Res* 2007; 35: 407–10.
 26. Colovos C, Yeates TO. Verification of protein structures: Patterns of nonbonded atomic interactions. *Protein Sci* 1993; 2: 1511–9.
 27. Gasteiger E, Hoogland C, Gattiker A, Duvaud S, Wilkins MR, Appel RD, et al. Protein identification and analysis tools on the ExPASy Server. In: John M. Walker, editor. *The proteomics protocols handbook*. Tatowa, NJ, USA: Humana Press 2005; p. 571–607.
 28. Dundas J, Ouyang Z, Tseng J, Binkowski A, Turpaz Y, Liang J. CASTp: Computed atlas of surface topography of proteins with structural and topographical mapping of functionally annotated residues. *Nucl Acids Res* 2006; 34: 116–8.
 29. Kawabata T, Go N. Detection of pockets on protein surfaces using small and large probe spheres to find putative ligand binding sites. *Proteins* 2007; 68: 516–29.
 30. Hillisch A, Pineda LP, Hilgenfeld R. Utility of homology models in the drug discovery process. *Drug Discov Today* 1994; 9(15): 659–69.

Correspondence to: Ozal Mutlu, Marmara University, Faculty of Arts and Sciences, Department of Biology, Goztepe Campus, 34722, Goztepe, Istanbul, Turkey.
E-mail: ozal.mutlu@marmara.edu.tr

Received: 28 September 2012

Accepted in revised form: 30 January 2013